Research paper

Effect of energetic nanocomposite powder additives on fuel drop autoignition

Fedor Frolov* and Sergey Frolov*†

*Department of Combustion and Explosion N. N. Semenov Institute of Chemical Physics Russian Academy of Sciences

4, Kosigin Street, Moscow 119991 RUSSIAN FEDERATION
TEL : +7−495− 9397228
†Corresponding address : sergei@frolovs.ru

Received : November 22, 2010 Accepted : February 20, 2011

Abstract

Recent experimental investigations showed that ultra-dispersed powders of mechanically activated nanocomposite Al −MoO_3 and Mg−MoO_3 particles exhibit anaerobic explosion-type reaction at relatively small heating up to 500−600 K. Therefore thickening of liquid hydrocarbons with such particles can be effectively used for mixture homogenization in transportation engines and decreasing pollutant emissions into the atmosphere. When placed into a hot gaseous flow, thickened-fuel drops can exhibit controlled 'microexplosion' behavior. In this paper, the possibility of thickened-fuel drop 'microexplosion' is examined using a mathematical model of single-component drop heating, evaporation, and combustion.

Keywords : liquid drop combustion, mechanically activated nanocomposite particles, 'microexplosion.'

1. Introduction

The object of the study reported herein is the liquid fuel drop thickened with energetic nanocomposite particles (Fig. 1). These particles are composed of metal (Aluminum, Magnesium, etc.) and solid oxidizer (Molybdenum oxide, Teflon, Carbon, etc.). The powder of such particles is prepared using mechanical activation technique (Fig. 2). Two powders (metal and oxidizer) are mixed and mechanically milled in a ball mill during a certain time. In the course of milling, one obtains energetic powder with metal and oxidizer particles in close contact with or encapsulated in each other.

Figure 3 shows the microphotographs of mechanically

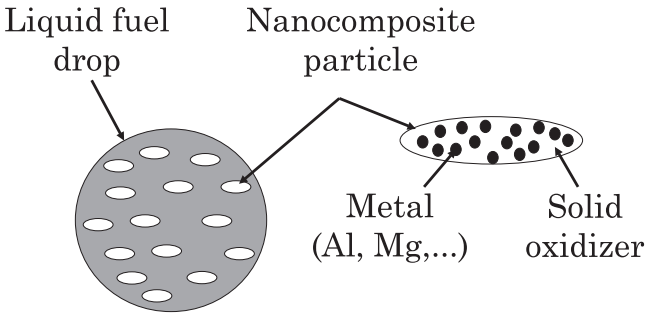

Fig. 1 Hydrocarbon fuel drop thickened with nanocomposite powder.

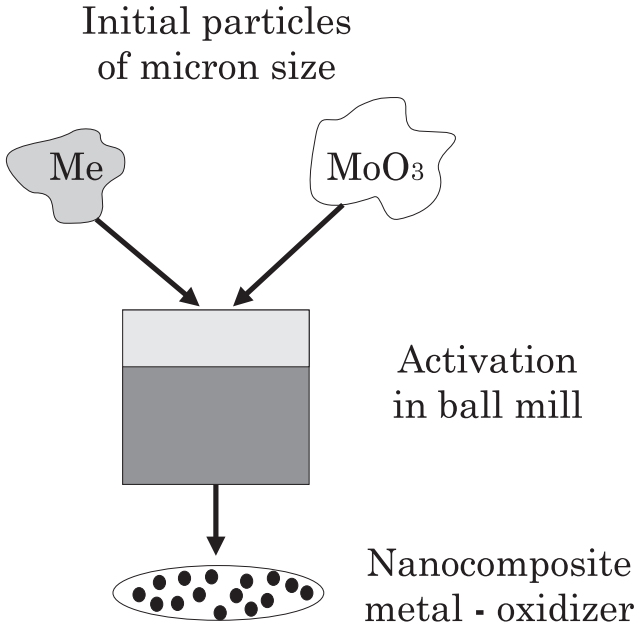

Fig. 2 Mechanical activation of powders.

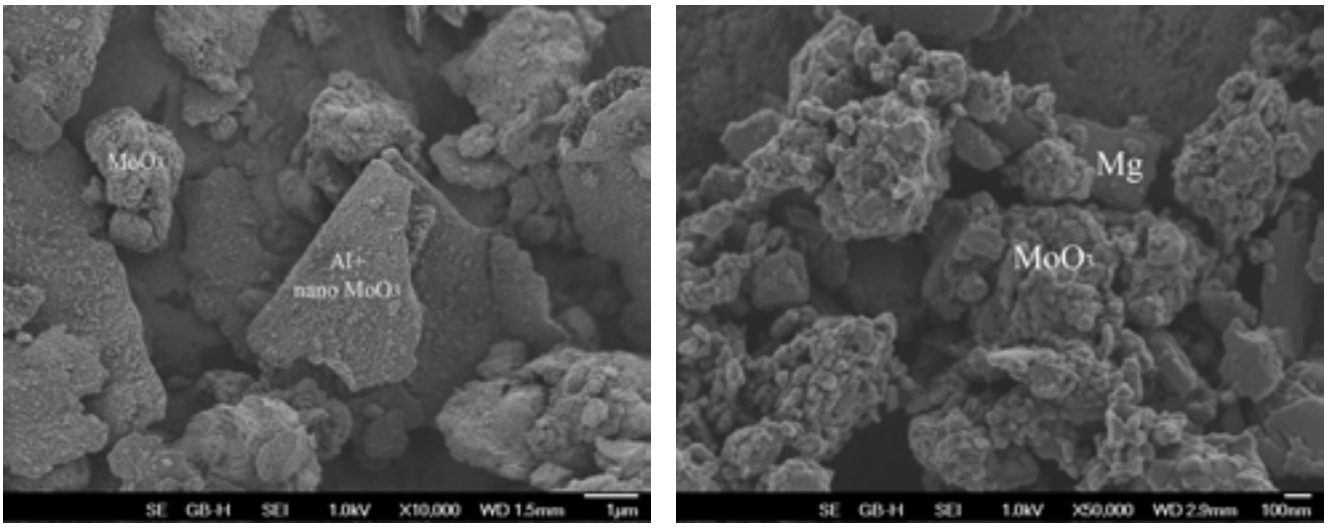

(a) (b)

Fig. 3 Microphotographs of mechanically activated Al−MoO_3(a) and Mg−MoO_3(b) nanocomposite powders prepared using mechanical activation technique.[1), 2)]

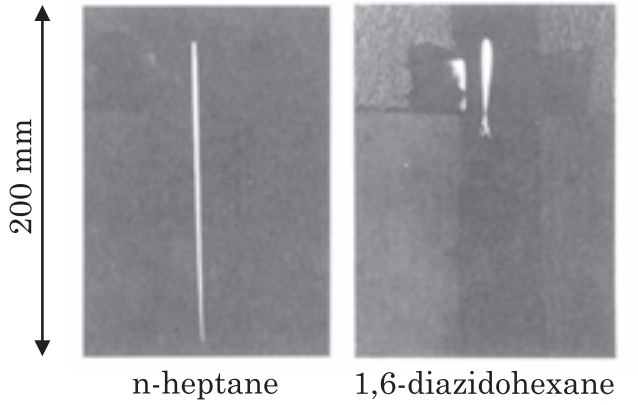

Fig. 4 Flame streak traced by the burning of the drop stream for different fuels, showing their relative burning intensities and tendencies to microexplode.[3)]

activated Al−MoO_3 (Fig. 3a) and Mg−MoO_3 (Fig. 3b) nanocomposite powders[1), 2)]. The Al−MoO_3 system contains Al flakes of micron size covered by MoO_3 nanoparticles. In Mg−MoO_3 system, the size of Mg particles is considerably smaller (about 200 nm) and the contact area between metal and oxidizer is considerably larger than in Al−MoO_3 system.

From now on, such powders will be referred to as energetic nanocomposite powders (ENP). Term "nanocomposite" comes from the fact that one or both ingredients are presented by nanosize particles. Such a powder is very reactive. Its relatively small heating results in explosion-like exothermic reaction.

The idea of the study reported herein was to find out whether addition of small amounts of such a powder to liquid fuel can lead to drop 'microexplosion.' To illustrate the drop 'microexplosion' phenomenon, we refer to Fig. 4[3)]. This figure shows time integrated flame streaks of the freely falling burning drops of ***n***-heptane and diazidohexane. The length of the flame streak is proportional to the drop burning time. Clearly, the lifetime of the second drop is a factor of 3 shorter, which is caused by explosion of the liquid high-explosive drop due to its heating followed by condensed-phase decomposition reactions. Similar 'microexplosions' of drops were observed for hydrocarbon fuel blends and emulsions (see, e.g., Lasheras et al.[4)]). The same drop behavior can be expected if one adds ENP to a hydrocarbon fuel.

2. Overview of previous experimental findings

In our preliminary experimental investigations[1)], powders of mechanically activated nanocomposite Al−MoO_3 and Mg−MoO_3 particles were shown to exhibit explosion-type anaerobic reaction at relatively small heating up to 500−600 K. The effect of ENP additive to hydrocarbon fuel is presented in Fig. 5. Figure 5 shows some experimental results for ignition delays of thickened ***n***-heptane and Diesel oil obtained in static apparatus. Circles and squares correspond to neat fuels. Triangles correspond to fuels with 2.5% (wt.) additive of energetic Mg−MoO_3 nanocomposite. One can see that ENP additive becomes effective starting from a certain threshold temperature (solid vertical line) which is about 550−570 K for Diesel oil. At temperatures exceeding the threshold value, the ignition delay drops abruptly by about 2 orders of magnitude.

The most important experimental findings reported by Borisov et al.[1)] are :

- even very small additives of ENP can significantly reduce ignition delays of hydrocarbon fuels ;
- at temperatures below the threshold value, the ignition delays of thickened fuels differ only insignificantly from the ignition delays of neat hydrocarbon fuels ;
- the threshold temperature is independent of the fuel type and is controlled by the ENP properties ; and
- burning velocities of thickened-fuel drop suspensions in air at elevated temperatures after their self-ignition in hot spots can be 1.5 to 2 order of magnitude greater than burning velocities of the appropriate hydrocarbon fuels under identical conditions. The flame in such suspensions propagates with acceleration, which would facilitate its

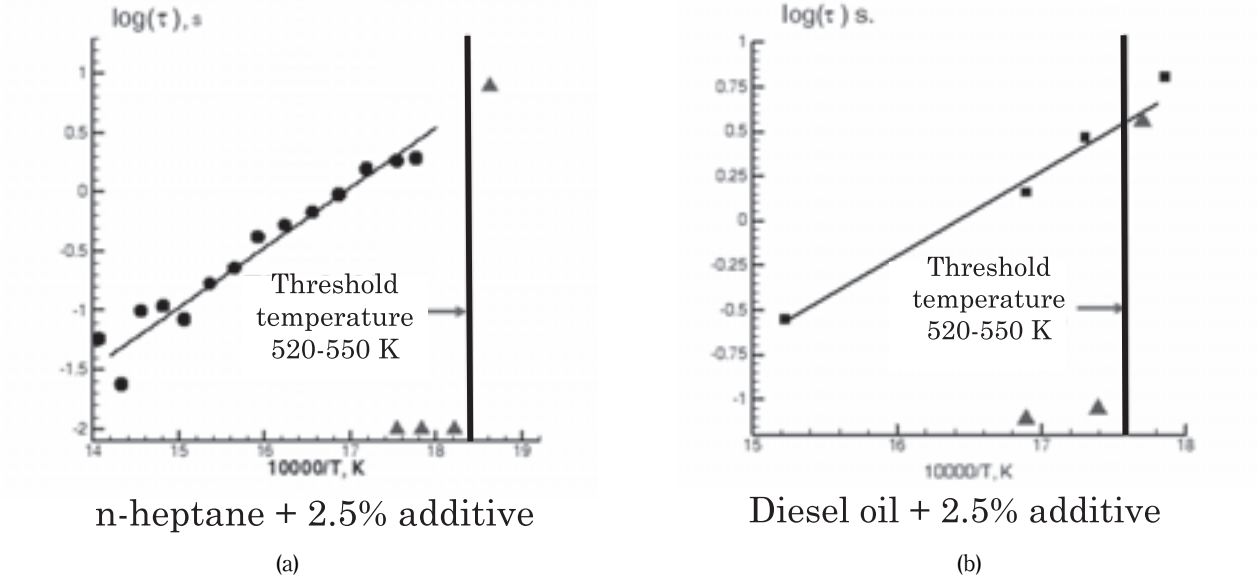

Fig. 5 Experimental results for ignition delays of neat (circles and squres) and thickened (triangles) *n*−heptane (a) and Diesel oil (b) measured in static apparatus.[1)]

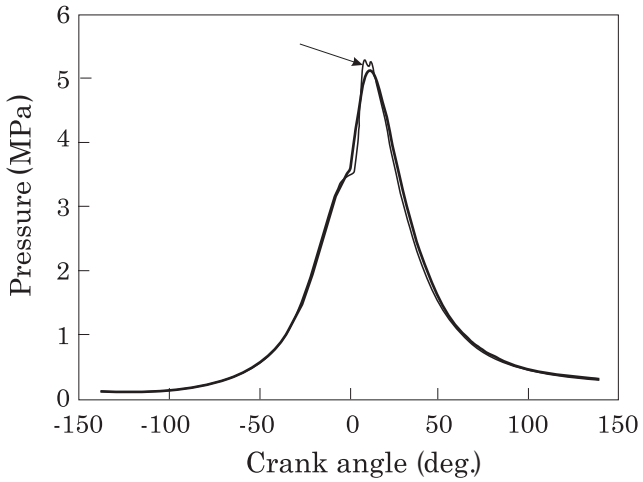

Fig. 6 Experimental indicating diagrams for engine operation with neat Diesel oil (thin solid curve shown by arrow) and with Diesel oil (thick solid curve) thickened with 1%, 2%, 3%, and 4% (wt.) Mg−MoO_3 nanocomposite additive.

run away to detonation.

In addition to the experiments in static apparatus, a series of experiments in research Diesel engine was made. The engine used was the four-cylinder air-cooled Diesel engine operating at a fixed rotation rate (1500 rpm). The engine was operated both with neat Diesel oil and with Diesel oil thickened with 1%, 2%, 3%, and 4% (wt.) Mg−MoO_3 nanocomposite additive. The most important findings are :

- the indicating efficiency of the engine operated with the thickened fuel increased by about 10%−11% as compared to operation with neat fuel ;
- the maximum indicating pressure decreased by about 4% as compared to operation with neat fuel irrespectively of the amount of ENP additive ; and
- the maximum rate of pressure rise decreased nearly twice as compared to operation with neat fuel.

These findings are illustrated by Fig. 6 which shows a set of experimental indicating diagrams for engine operation with neat Diesel oil (thin solid curve marked by arrow) and with thickened Diesel oil (thick solid curve enveloping indicating diagrams for fuel with 1%, 2%, 3%, and 4% (wt.) Mg−MoO_3 nanocomposite additive).

In view of these experimental findings, we studied the possibility of thickened-fuel drop 'microexplosion' using a mathematical model[5)] of single-component drop heating, vaporization, ignition and combustion. At this stage of investigation, the effect of ENP additive on fuel drop behavior was neglected.

3. Model

The liquid drop is assumed to be a sphere of radius r_s and occupy the region $0 < r < r_s$ at time t. The droplet size is allowed to vary in time due to thermal expansion and liquid vaporization processes. Therefore, r_s is treated as the moving boundary. The continuity equation for liquid is

$$\frac{\partial \rho_d}{\partial t}+\frac{1}{r^2}\frac{\partial}{\partial r}(r^2\rho_d u_d)=0$$

where index d relates to liquid, r is the radial coordinate, ρ is the density, and u is the velocity.

Temperature distribution in liquid ($0 < r < r_s$), $T_d(r)$ is governed by the energy equation :

$$c_d\rho_d\frac{\partial T_d}{\partial t}+c_d\rho_d u_d\frac{\partial T_d}{\partial r}=\frac{1}{r^2}\frac{\partial}{\partial r}\left(\lambda_d r^2\frac{\partial T_d}{\partial r}\right),$$

$$T_d(0,r)=T_{d0},\ \left.\frac{\partial T_d}{\partial r}\right|_{r=0}=0,\ T_d(t,r_s)=T_g(t,r_s),$$

where T is the temperature, c is the specific heat, and λ is the thermal conductivity.

The mass concentration of liquid vapor (index v) at the drop surface is

$$Y_v=\frac{P_v}{P}\frac{W_v}{W},$$

where P is the pressure, W is the molecular mass, and bar denotes the mean value.

The gas phase (index g) is assumed to occupy region $r_s < r < R$, where R is the half-distance between drops in gas–drop suspension. The gas flow around the drop is governed by the continuity equation

$$\frac{\partial \rho_g}{\partial t} + \frac{1}{r^2}\frac{\partial}{\partial r}(r^2 \rho_g u_g) = 0,$$

$$\rho_d \left(u_d - \frac{\partial r_s}{\partial t}\right)\Big|_{r=r_s} = \rho_g \left(u_g - \frac{\partial r_s}{\partial t}\right)\Big|_{r=r_s},$$

species continuity equation

$$\rho_g \frac{\partial Y_j}{\partial t} = \frac{1}{r^2}\frac{\partial}{\partial r}(\rho_g r^2 Y_j V_j) - \rho_g u_g \frac{\partial Y_g}{\partial r} + \omega_{gj}$$

$$Y_j(0,r) = Y_{j0}, \quad j = 1,2,...,N,$$

$$-\rho_d u_i \beta_j|_{r=r_s} = \rho_g Y_j \left(u_g - \frac{\partial r_m}{\partial t}\right) + \rho_g Y_j V_j\Big|_{r=r_s},$$

$$\frac{\partial \overline{W} Y_j}{\partial r}\Big|_{r=R} = 0, \quad j = 1,...,N$$

$$X_j = Y_j \overline{W} / W_j$$

$$\frac{\partial X_j}{\partial r} = \sum_{k=1}^{N}\left(\frac{X_j X_k}{D_{jk}}\right)(V_k - V_j)$$

$$\omega_{gj} = W_{gj} \sum_{k=1}^{L} (\nu''_{j,k} - \nu'_{j,k}) A_k T_g^{n_k} \exp\left(-\frac{E_k}{RT_g}\right) \prod_{l=1}^{N}\left(\frac{Y_{gl}\rho_g}{W_{gl}}\right)^{\nu'_{l,k}}$$

$$\beta_j = 1 \text{ at } j = v$$

$$\beta_j = 0 \text{ at } j \neq v$$

and energy equation

$$c_{pg}\rho_g \frac{\partial T_g}{\partial t} = \frac{1}{r^2}\frac{\partial}{\partial r}\left(\lambda_g r^2 \frac{\partial T_g}{\partial r}\right) - c_{pg}\rho_g u_g \frac{\partial T_g}{\partial r} + \Omega$$

$$T_g(0,r) = T_{g0}$$

$$T_g(t,r_s) = T_d(t,r_s), \frac{\partial T_g}{\partial r}\Big|_{r=R} = 0$$

$$\Omega = \sum_{k=1}^{L} H_k A_k T_g^{n_k} \exp\left(-\frac{E_k}{RT_g}\right) \prod_{j=1}^{N}\left(\frac{Y_{gj}\rho_g}{G_{gj}}\right)^{\nu'_{j,k}},$$

where index 0 denotes the initial value, Y_j is the mass fraction of species j; D_j is the diffusion coefficient for species j; ω_j is the rate of variation of mass fraction of species j due to chemical reactions; Ω is the chemical heat source; A_k, n_k, E_k, and H_k are the preexponential factor, power exponent, activation energy, and heat effect of the kth reaction; N is the number of species; L is the number of reactions, respectively.

In addition to above equations, the boundary condition for tailoring temperature fields in liquid and gas at $r = r_s$

$$\lambda_d \frac{\partial T_d}{\partial r} - \frac{\rho_{di} u_i L_v}{W_v} = \lambda_g \frac{\partial T_g}{\partial r},$$

equation of state for the gas phase

$$\rho_g = \frac{P\overline{W}}{R^o T_g},$$

and the condition of constant pressure

$$P = P_0 = const$$

are specified. Here, L_v is the latent heat of vaporization and R^o is the universal gas constant.

Molecular transport processes in liquid and gas phases as well as the corresponding specific heats are taken from Reid et al.[6]

To study ignition and combustion of hydrocarbon fuel drops in air and oxygen, the overall 5-step oxidation mechanism[5] for *n*-tetradecane and *n*-dodecane was used.

The set of governing equations was integrated numerically using nonconservative finite-difference scheme and adaptive moving grid. The computational error was continuously monitored by checking balances of C and H atoms as well as energy balance at each time step.

4. Results of calculations

In the calculations, ignition procedure simulated the ignition process in Diesel engines or behind shock waves, i. e., fuel drops were instantaneously placed in hot air or oxygen initially at temperature T_{g0} and pressure P_0. Two sets of calculations were made for *n*-tetradecane and *n*-dodecane drops of different initial radii r_{s0} at different T_{g0} and P_0. The results of calculations for *n*-heptane were reported earlier.[7]

Intuitively, the necessary condition for microexplosion is the requirement for the liquid temperature to reach the characteristic explosion temperature (~570K for Mg–MoO_3 additive) of ENP. However the model does not provide the sufficient conditions for drop microexplosion. Therefore it was instructive to estimate the characteristic times taken for the drop surface (time τ_s) and drop center (time τ_c) to reach this explosion temperature threshold. Given these estimates, one can at least expect that the probability of drop microexplosion increases with time within interval $\tau_s \le t < \tau_c$ whereas at $t \ge \tau_c$ the microexplosion is getting inevitable. The latter is of course valid only if τ_c is less than the drop lifetime.

As an example, Figs. 7 and 8 show the predicted time histories of temperature at the *n*-tetradecane drop surface (solid curves) and in the drop center (dashed curves) at P_0 =10 bar (Fig. 7) and 20 bar (Fig. 8) and air temperature 900 K (characteristic of Diesel engine). Tetradecane was used to simulate Diesel oil.

At pressure 10 bar, liquid reaches the characteristic explosion temperature (~570K for Mg–MoO_3 additive) of ENP only at the end of drop lifetime. At pressure 20 bar, the times taken for the *n*-tetradecane drop to heat up to the characteristic ENP explosion temperature vary from τ_s = 0.2 ms (near-surface liquid layers) to τ_c = 0.9 ms (drop center). At higher pressures, these times are getting

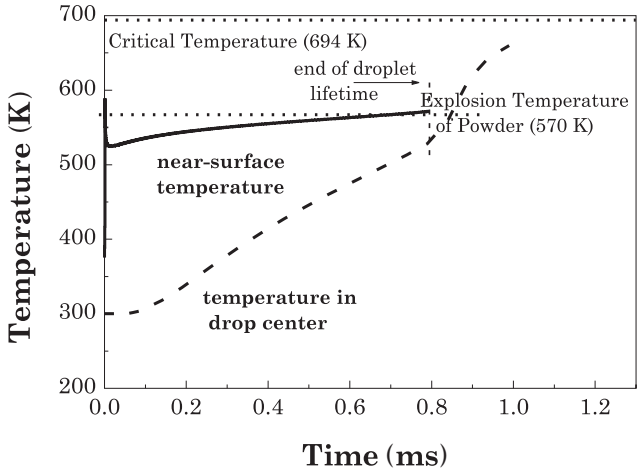

Fig. 7 Predicted histories of gas temperature at the surface of burning *n*−tetradecane drop (solid curve) and liquid temperature in the drop center (dashed curve) at pressure 10 bar (r_{s0} =15μm, T_{g0} = 900K).

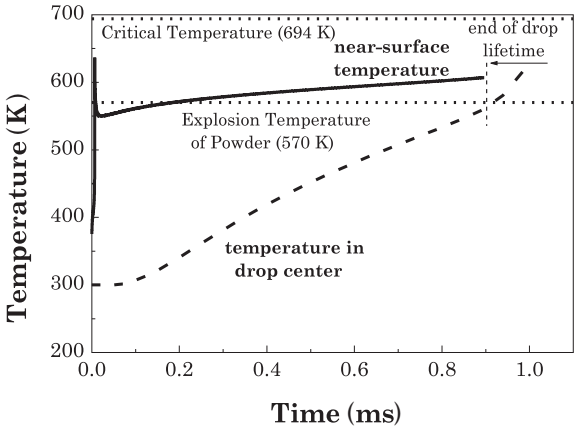

Fig. 8 Predicted histories of gas temperature at the surface of burning *n*−tetradecane drop (solid curve) and liquid temperature in the drop center (dashed curve) at pressure 20 bar (r_{s0} =15μm, T_{g0} = 900K).

shorter. These results are directly relevant to the behavior of thickened-fuel drops of Diesel oil in Diesel engine (see above) and demonstrate a possibility of drop 'microexplosion' during engine operation.

Similar calculations were made for the conditions realized behind strong shock waves propagating at Mach number M in *n*-dodecane drop suspensions in gaseous oxygen. Dodecane was used to simulate liquid rocket propellant (kerosene).[8] These calculations were aimed at determining the conditions when ENP can effectively influence ignition of hydrocarbon fuel drops in oxygen. The example of the resultant "Shock wave Mach number M−Initial drop diameter d_{s0}" diagram for *n*-dodecane drop suspensions is presented in Fig. 9. This diagram identifies the M−d_{s0} parametric domain where Mg−MoO_3 ENP additive is capable of inducing *n*-dodecane drop 'microexplosion' in a drop suspension of stoichiometric composition behind a shock wave at P_0=1 bar and T_{g0} = 293 K in gaseous oxygen. In the parametric domain A, the drop center is heated to the threshold temperature of ~ 570K during less than 100 μs after shock loading (i.e., $\tau_c < 100\mu s$), whereas in the parametric domain B, the drop surface temperature attains the threshold value less than

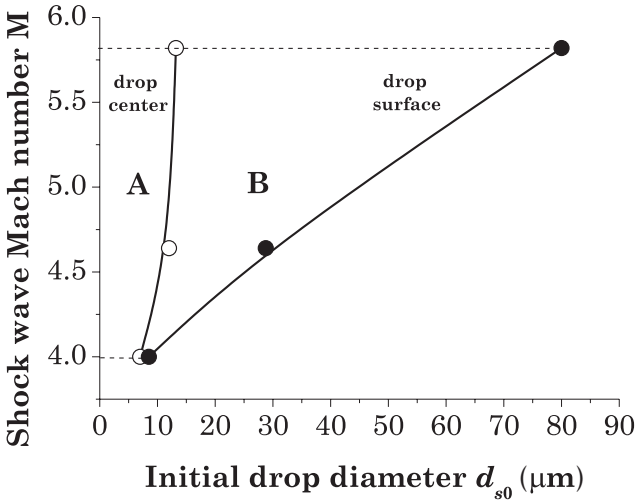

Fig. 9 "Shock wave Mach number M−Initial drop diameter d_{s0}" diagram for *n*−dodecane drop suspensions in gaseous oxygen. In parametric domain A, drop center is heated to the threshold temperature of ~570 K faster than 100 μs after shock loading. In parametric domain B, the drop−surface temperature attains the threshold value less than in 100 μs after shock loading.

in 100 μs after shock loading (i.e., $\tau_s < 100\mu s$). The "100 μs" criterion is used here to characterize detonability limits of drop suspensions.[9]

The diagram of Fig. 9 clearly indicates that even very small drops 10 μm in diameter are capable of supporting detonations in neat-fuel drop suspensions. Addition of Mg −MoO_3 ENP to liquid propellant can considerably widen detonability limits due to 'microexplosion' of thickened-fuel drops.

Concluding remarks

Characteristic times of thickened-fuel drop 'microexplosion' have been estimated based on the mathematical model of liquid drop heating, vaporization, ignition, and combustion. It has been shown that in Diesel engine conditions, thickened-fuel drops most probably exhibit ' microexplosion' phenomenon. Drop 'microexplosion' could be a reason of increased engine efficiency due to mixture homogenization in our experiments reported earlier.

Fuel thickening with ENP can be used for arranging the operation process in a pulse-detonation liquid-propellant rocket engine. It has been shown that addition of ENP to liquid propellant can considerably widen detonability limits due to controlled drop 'microexplosion'.

The results of this study are also relevant to safety issues in process industries. They demonstrate that the mixtures of liquid hydrocarbons with negligibly small amounts of reactive powders capable of anaerobic chemical transformation can potentially exhibit a significant explosion hazard.

Acknowledgments

This work was supported by the Federal special purpose program "Scientific and teaching human resources of innovative Russia" for 2009−2013 (State contract #П502), Federal special purpose program

"Research and development in priority directions of technological complex of Russia" (State contract # 02.516.12.6026), Federal special purpose program "Nanotechnologies 2009–2012" (State contract #019-600/2009), and Russian Foundation for Basic research (grant # 08-08-00068).

References

1) A. A. Borisov, I. V. Kolbanev, A. N. Streletskii, K. Ya. Troshin, S. M. Frolov, and F. S. Frolov, In: "Combustion and Explosion" (S. M. Frolov, editor), Moscow: Torus Press, p. 118 (2010).
2) S. M. Frolov, A. A. Borisov, I. V. Kolbanev, A. N. Streletskii, and K. Ya. Troshin, Patent of Russian Federation disclosure #2010126772 dated 01.07.2010.
3) C. K. Law, In: "Propulsion Combustion: Fuels to Emissions" (G. D. Roy, editor), N.Y., Taylor and Francis, pp. 63–92 (1998).
4) J. C. Lasheras, A. C. Fernandes-Pello, and F. L. Dryer, Proc. Combustion Institute, 18, pp. 293–305, The Combustion Institute, Pittsburgh (1981).
5) S. M. Frolov, V. Ya. Basevich, F. S. Frolov, A. A. Borisov, V. A. Smetanyuk, K. A. Avdeev, and A. N. Hotz, Rus. J. Chemical Physics, 28, 5, 3 (2009).
6) R. C. Reid, J. M. Prausnitz, and T. K. Sherwood, "The Properties of Gases and Liquids," N.Y., McGrow–Hill (1977).
7) F. S. Frolov and S. M. Frolov, In, "Combustion and Explosion" (S. M. Frolov, editor), Moscow, Torus Press, p. 124 (2010).
8) S. M. Frolov, Pulse Detonation Engines, Moscow, Torus Press (2006).
9) V. Ya. Basevich, S. M. Frolov, and V. S. Posvyanskii, Rus. J. Chemical Physics, 24, 7, 60 (2005).